Journal of Physics: Conference Series

PAPER • OPEN ACCESS

Towards prediction of the rates of antihydrogen positive ion production in collision of antihydrogen with excited positronium

To cite this article: T Yamashita *et al* 2020 *J. Phys.: Conf. Ser.* **1412** 052012

Towards prediction of the rates of antihydrogen positive ion production in collision of antihydrogen with excited positronium

T Yamashita[1,2], Y Kino[2], E Hiyama[1,3], K Piszczatowski[4], S Jonsell[5], P Froelich[4]

[1]Nishina Center, RIKEN, Wako, 351-0198, Japan
[2]Department of Chemistry, Tohoku University, Sendai, 980-8578, Japan
[3]Department of Physics, Kyushu University, Fukuoka, 819-0395, Japan
[4]Department of Chemistry, Uppsala University, Uppsala, Box 518 751-20, Sweden
[5]Department of Physics, Stockholm University, Stockholm, SE-10691, Sweden

E-mail: takuma.yamashita@riken.jp

Abstract. We present a 4-body calculation of scattering between an antihydrogen atom ($\bar{H}$) and a positronium (Ps) aiming at the prediction of cross sections for the production of antihydrogen positive ions ($\bar{H}^+$). The antihydrogen positive ions are expected to be a useful source of ultra-cold anti-atoms for the test of matter-antimatter gravity. We convert the Schrödinger equation to a set of coupled integro-differential equations that involve intermediate states which facilitate the internal region description of the scattering wavefunction. They are solved using a compact finite difference method. Our framework is extended to scattering between an excited Ps and $\bar{H}$. Cross sections of the reactions, Ps (1s/2s/3s) + $\bar{H} \rightarrow e^- + \bar{H}^+$, in s-wave collisions, are calculated. It is found that the reactions originating from Ps (1s/2s) + $\bar{H}$ produce $\bar{H}^+$ with a constant cross section within 0.05 eV above the threshold while the reaction cross section from Ps (3s) decreases as the collision energy increases in the same energy interval. Just above the threshold, the cross section of $\bar{H}^+$ production from Ps (3s) + $\bar{H}$ in s-wave collision is 7.8 times larger than that from Ps (1s) + $\bar{H}$ in s-wave and 2.3 times larger than that from Ps (2s) + $\bar{H}$ in s-wave. The near-threshold de-excitation reaction from Ps (3s) + $\bar{H}$ occurs more rapidly than the $\bar{H}^+$ production.

1. Introduction

The antihydrogen atom ($\bar{H}$), consisting of an antiproton ($\bar{p}$) and a positron (e^+), is a good probe for CPT symmetry and for physics beyond the standard model. Experimental development of sources of cold antihydrogen atoms [1–7] is aimed at a precise measurement of energy levels of $\bar{H}$ and spectroscopy of $\bar{H}$ has been reported recently [8–10].

Another application of the cold antihydrogen atoms is measurement of gravitational properties of antimatter [11] testing the weak equivalence principle. Some experiments have been planned to study the gravitational properties of $\bar{H}$ [12–22]. The antihydrogen positive ion ($\bar{H}^+ = \bar{p}e^+e^+$) may be manipulated by electric fields and be used in studies of particle physics and atomic physics. $\bar{H}^+$ ions are expected to be useful intermediates in the production of antihydrogen atoms [16, 17]. It would be prepared by sympathetic cooling of $\bar{H}^+$ (with Be^+ ions) and the subsequent positron detachment. $\bar{H}^+$ can also be utilized to develop an energy-tunable antihydrogen beam that will be used in atomic collision experiments.

Reaction between positronium (Ps = e^+e^-) and antihydrogen atom ($\bar{H}$ = $\bar{p}e^+$) has been featured recently as one of the promising production schemes of $\bar{H}^+$. A channel of $\bar{H}^+$ production,

$$\mathrm{Ps}\ (1s) + \bar{\mathrm{H}}\ (1s) \rightarrow e^- + \bar{H}^+, \tag{1}$$

opens at the collision energy 6.05 eV in the center-of-mass system. A reaction between the second excited Ps ($n = 3$) and $\bar{H}$ (1s) is also promising because the positron transfer to $\bar{H}$ from Ps ($n = 3$),

$$\mathrm{Ps}\ (n = 3) + \bar{\mathrm{H}}\ (1s) \rightarrow e^- + \bar{H}^+, \tag{2}$$

can occur from the collision energy 1.7 meV. The low-energy collision between Ps ($n = 3$) and $\bar{H}$ (1s) resulting in $\bar{H}^+$ production has been expected to have large cross sections [23–25]; however, these rearrangement reactions compete with several inelastic reactions of Ps (de-)excitation and require rigorous theoretical treatment.

The Ps-$\bar{H}$ system is the charge-conjugate system of Ps-H. Low-energy scattering of Ps (1s) by H has been studied in several works as one of the most fundamental scattering problems for the investigation of positronium-atom interaction [26–29]. A number of theoretical studies have produced H (1s) + Ps (1s) total/differential cross sections and scattering length [30–38]. On the other hand, the investigation of inelastic scattering has been limited to calculations using methods suitable for intermediate or high-energy collisions [23, 25, 39]. Calculations based on the close-coupling method [35, 40, 41] were performed to study slow inelastic collisions; however, the information on the reaction branches including a rearrangement reaction channel, namely $\bar{H}^+$ production channel, is still limited.

This work presents a four-body calculation of Ps-$\bar{H}$ scattering with an open channel of $e^- + \bar{H}^+$ as well as all possible competing inelastic channels. We revise our previous pilot calculation [42] and extend the method to scattering of excited Ps by $\bar{H}$. Numerical results are reported for s-wave collision between Ps (1s/2s/3s) and $\bar{H}$ (1s). Atomic units (a.u.; $m_e = \hbar = e = 1$) are used throughout this paper, except where mentioned otherwise.

2. Theory

In this paper we consider a reaction of Ps ($n_0 l_0$) + $\bar{H}$ (1s) resulting in Ps ($n'l'$) + $\bar{H}$ (1s) or $e^- + \bar{H}^+$. For simplicity, we denote the two positrons with e_1^+ and e_2^+. The Schrödinger equation for the scattering state is written as

$$(H - E)\Psi = 0, \tag{3}$$

where the Hamiltonian H includes kinetic energy operators and all inter-particle Coulomb potential interactions expressed in the center-of-mass coordinate system.

The whole system can be characterized by its parity P, a total angular momentum J and its projection onto z-axis M, where the z-axis can be chosen to be in an arbitrary direction. The $\bar{H}^+$ production channel, $e^- + \bar{H}^+$, can open when the two positrons form a spin singlet under the Coulombic interactions. The ground state of $\bar{H}^+$ possesses positive parity and zero angular momentum in total; therefore, the parity of the $\bar{H}^+$ production channel is characterized by the angular momentum between e^- and $\bar{H}^+$. The parity satisfies $P = (-1)^J$, which means the antihydrogen positive ion production channel opens only in natural parity. The channels of Ps (nl) + $\bar{H}$ (1s) can be distinguished by a set of quantum numbers $\alpha \equiv \{n, l, \lambda\}$ for a given J and M, where λ is the angular momentum of the scattering partial wave and satisfies a condition of natural parity, $(-1)^{l+\lambda} = (-1)^J$. We denote the initial channel as $\alpha_0 \equiv \{n_0, l_0, \lambda_0\}$.

We construct the total wavefunction Ψ in equation (3) as

$$\Psi = \sum_\alpha \psi_\alpha + \sum_\upsilon b_\upsilon \Phi_\upsilon, \tag{4}$$

where Φ_υ describe the intermediate, square-integrable states of the scattering (obtained by the diagonalization of the full 4-body Hamiltonian, see below), b_υ are the expansion coefficients, and ψ_α

are the channel functions that describe the asymptotic behavior of the initial/final states. $\psi_\alpha(\mathbf{r},\mathbf{R},\boldsymbol{\rho})$ for Ps (nl) + $\bar{\mathrm{H}}$ (1s) is written as

$$\psi_\alpha(\mathbf{r},\mathbf{R},\boldsymbol{\rho}) = \frac{1}{\sqrt{2}}\left\{\mathcal{R}^{\mathrm{Ps}}_{nl}(r)\mathcal{R}^{\bar{\mathrm{H}}}_{1\mathrm{s}}(R)\mathcal{R}_\alpha(\rho)\left[Y_l(\hat{\mathbf{r}})Y_\lambda(\hat{\boldsymbol{\rho}})\right]_{JM} + (1 \leftrightarrow 2)\right\}, \tag{5}$$

where $\left[Y_l(\hat{\mathbf{r}})Y_\lambda(\hat{\boldsymbol{\rho}})\right]_{JM} = \sum_{m_l}\sum_{m_\lambda} C(lm_l\lambda m_\lambda|JM)Y_{lm_l}(\hat{\mathbf{r}})Y_{\lambda m_\lambda}(\hat{\boldsymbol{\rho}})$ with $C(lm_l\lambda m_\lambda|JM)$ the Clebsh-Gordan coefficients. $(1 \leftrightarrow 2)$ is a term where two positrons are exchanged. Since we consider the spin singlet, the spatial part should be symmetrized and thus $(1 \leftrightarrow 2)$ is added in the positive sign. $\mathbf{r}$, $\mathbf{R}$ and $\boldsymbol{\rho}$ are relative vectors from e^- to e^+_1, from $\bar{\mathrm{p}}$ to e^+_2, and from the center-of-mass of Ps to that of $\bar{\mathrm{H}}$, respectively. $\mathcal{R}^{\mathrm{Ps}}_{nl}(r)$, $\mathcal{R}^{\bar{\mathrm{H}}}_{1\mathrm{s}}(R)$ and $\mathcal{R}_\alpha(\rho)$ are radial functions of Ps (nl), $\bar{\mathrm{H}}$ (1s), and the relative motion between them, respectively. It should be noted that the spherical harmonics of $\bar{\mathrm{H}}$ (1s), $Y_{00}(\hat{\mathbf{R}}) = 1/\sqrt{4\pi}$, is included in $\mathcal{R}^{\bar{\mathrm{H}}}_{1\mathrm{s}}(R)$ for brevity. The channel function for e^- + $\bar{\mathrm{H}}^+$ is written as

$$\psi_\alpha(\mathbf{r}',\mathbf{R}',\boldsymbol{\rho}') = \phi^{\bar{\mathrm{H}}^+}_{\Lambda=0}(\mathbf{r}',\mathbf{R}')\mathcal{R}_\alpha(\rho')Y_{JM}(\hat{\boldsymbol{\rho}}'), \tag{6}$$

where $\phi^{\bar{\mathrm{H}}^+}_{\Lambda=0}$ is a three-body wavefunction of $\bar{\mathrm{H}}^+$ that includes the exchange terms and $\mathcal{R}_\alpha$ is a radial function of the relative motion between e^- and $\bar{\mathrm{H}}^+$. $\phi^{\bar{\mathrm{H}}^+}_{\Lambda=0}$ reproduces the three-body energy of $\bar{\mathrm{H}}^+$ as $-0.527\,445$ a.u. which differs by $0.000\,001$ a.u. from the best variational result. $\mathbf{r}'$, $\mathbf{R}'$ and $\boldsymbol{\rho}'$ are relative vectors from $\bar{\mathrm{p}}$ to e^+_1, from the center-of-mass of $(\bar{\mathrm{p}},\mathrm{e}^+_1)$ to e^+_2, and from the center-of-mass of $\bar{\mathrm{H}}^+$ to e^-, respectively. $\Lambda = 0$ means the $\bar{\mathrm{H}}^+$ has zero total angular momentum.

This expression of the scattering state is basically the same as the one used in three-body muonic atom collisions [43,44] and recently used in four-body antihydrogen atom collisions [42,45]. Functions Φ_υ are expanded in finite range Gaussian functions and diagonalize the Hamiltonian according to $H\Phi_\upsilon = E_\upsilon\Phi_\upsilon$ with conditions $\langle\Phi_{\upsilon'}|\Phi_\upsilon\rangle = \delta_{\upsilon'\upsilon}$ and $\langle\Phi_{\upsilon'}|H|\Phi_\upsilon\rangle = E_\upsilon\delta_{\upsilon'\upsilon}$. The Schrödinger equation (3) is converted to a set of coupled equations with the following conditions, $\langle\mathcal{R}^{\mathrm{Ps}}_{nl}(r)\mathcal{R}^{\bar{\mathrm{H}}}_{1\mathrm{s}}(R)\left[Y_l(\hat{\mathbf{r}})Y_\lambda(\hat{\boldsymbol{\rho}})\right]_{JM}|H-E|\Psi\rangle_{\mathbf{r},\mathbf{R},\hat{\boldsymbol{\rho}}} = 0$, $\langle\phi^{\bar{\mathrm{H}}^+}_{\Lambda=0}(\mathbf{r}',\mathbf{R}')Y_{JM}(\hat{\boldsymbol{\rho}}')|H-E|\Psi\rangle_{\mathbf{r}',\mathbf{R}',\hat{\boldsymbol{\rho}}'} = 0$, and $\langle\Phi_\upsilon|H-E|\Psi\rangle = 0$. Here, $\langle\cdots\rangle_{\mathbf{r},\mathbf{R},\hat{\boldsymbol{\rho}}}$ means the integration over these coordinates leaving out integration over ρ. Expressing the radial functions of the relative motion in initial and final channels as $\mathcal{R}_\alpha(\rho) = \chi_\alpha(\rho)/\rho$, we obtain a set of coupled integro-differential equations for the channel functions, χ_α, that allow simultaneous determination of the expansion coefficients b_υ. We solve it by a compact finite difference method [46] under proper boundary conditions at $\rho \to \infty$

$$\chi_\alpha(\rho) \to \rho h^{(-)}_\lambda(k_\alpha\rho)\delta_{\alpha\alpha_0} - \sqrt{\frac{\upsilon_{\alpha_0}}{\upsilon_\alpha}}S_{\alpha\alpha_0}\rho h^{(+)}_\lambda(k_\alpha\rho) \tag{7}$$

for the initial channel α_0 and final channels dissociating into Ps (nl) and $\bar{\mathrm{H}}$ (1s). For the final channel dissociating into e^- + $\bar{\mathrm{H}}^+$, at $\rho' \to \infty$,

$$\chi_\alpha(\rho') \to -\sqrt{\frac{\upsilon_{\alpha_0}}{\upsilon_\alpha}}S_{\alpha\alpha_0}\rho' H^{(+)}_J(k_\alpha\rho'). \tag{8}$$

$h^{(\mp)}_\lambda$ is an incoming/outgoing spherical Hankel function and $H^{(\mp)}_\lambda$ an incoming/outgoing spherical Coulomb-Hankel function. υ_α is a speed of the relative motion between the fragments in channel α. The S-matrix elements $S_{\alpha\alpha_0}$ give partial cross sections $\sigma_{\alpha\alpha_0} = (2J+1)\pi|\delta_{\alpha\alpha_0} - S_{\alpha\alpha_0}|^2/k^2_{\alpha_0}$.

3. Results and discussion

Table 1. List of channels α = 1-7 in $J = 0$ opening just above the $e^- + \bar{H}^+$ dissociation threshold. In α = 1-6, the $\bar{H}$ is in 1s state.

	$\alpha = 1$	$\alpha = 2$	$\alpha = 3$	$\alpha = 4$	$\alpha = 5$	$\alpha = 6$	$\alpha = 7$
fragments	Ps (1s)+$\bar{H}$	Ps (2s)+$\bar{H}$	Ps (2p)+$\bar{H}$	Ps (3s)+$\bar{H}$	Ps (3p)+$\bar{H}$	Ps (3d)+$\bar{H}$	e^-+$\bar{H}^+$
partial wave	s-wave	s-wave	p-wave	s-wave	p-wave	d-wave	s-wave

Construction of the intermediate states $\{\Phi_\upsilon\}$ plays a primary role in accurate determination of the cross section. In this work we construct $\{\Phi_\upsilon\}$ using a Gaussian expansion method (GEM) [47–49], in terms of radial Gaussian functions and spherical harmonics, according to

$$\begin{aligned}\Phi_\upsilon &= \sum_{c=1}^{3}\sum_{n_c N_c \nu_c}\sum_{l_c L_c \lambda_c} A^{(\upsilon)}_{c n_c N_c \nu_c l_c L_c \lambda_c}\left\{ r_c^{l_c} R_c^{L_c} \rho_c^{\lambda_c} \exp\left(-\frac{r_c^2}{r_{n_c}^2} - \frac{R_c^2}{R_{N_c}^2} - \frac{\rho_c^2}{\rho_{\nu_c}^2}\right)\right. \\ &\times \left.\left[\left[Y_{l_c}(\hat{\mathbf{r}}_c) Y_{L_c}(\hat{\mathbf{R}}_c)\right]_{\Lambda_c} Y_{\lambda_c}(\hat{\boldsymbol{\rho}}_c)\right]_{JM} + (1 \leftrightarrow 2)\right\}, \end{aligned} \tag{9}$$

where $\{\mathbf{r}_c, \mathbf{R}_c, \boldsymbol{\rho}_c\}$ is a set of Jacobian coordinates (see figure 1). The first coordinate set $c = 1$ is best suited to describe the four-body interactions in the Ps + $\bar{H}$ configuration and $c = 2$ and $c = 3$ are best suited to describe the four-body interactions in the $e^- + \bar{H}^+$ configuration. The linear coefficients $A_{c n_c N_c \nu_c l_c L_c \lambda_c}$ are determined by diagonalizing the Hamiltonian H in the Gaussian basis set specified in equation (9). The non-linear coefficients $\{r_{n_c}\}$, $\{R_{N_c}\}$ and $\{\rho_{\nu_c}\}$ are distributed according to a geometrical progression between chosen minimum and maximum values. The relative motion between Ps and $\bar{H}$ for $c = 1$ and that between e^- and $\bar{H}^+$ for $c = 2$ and $c = 3$ are described in terms of $\{\rho_{\nu_c}\}$.

We proceed with the discussion on the s-wave collision between Ps (ns) + $\bar{H}$ (1s) ($n \leq 3$) resulting in $e^- + \bar{H}^+$. The whole system is $J = 0$ and all open channels α = 1-7 just above the $e^- + \bar{H}^+$ dissociation threshold are listed in table 1. The maximum range of the $\{\rho_{\nu_c}\}$ is chosen to be 40 a.u. for $c = 1$ and 110 a.u. for $c = 2$ and $c = 3$. Each function Φ_υ is described in 44320 Gaussian basis functions. It should be emphasized that each of the functions in the set $\{\Phi_\upsilon\}$ contains contributions expressed in several sets of Jacobian coordinates, namely those natural for the initial channel, the final channel, all energetically opened channels and also the important virtual excitation channels [41].

The antihydrogen positive ion production cross sections ($\sigma_{\rm ion}$) of the s-wave collision of Ps (ns) + $\bar{H}$ (1s) are presented in figure 2. The energy of the scattering is expressed in two ways: as the relative collision energy being $E - \epsilon_{\rm Ps} - \epsilon_{\bar{\rm H}}$ and as the antihydrogen impact energy on a Ps target at rest being $(E - \epsilon_{\rm Ps} - \epsilon_{\bar{\rm H}}) m_{\bar{\rm H}}/m_{\rm Ps}$, where $\epsilon_{\rm Ps}$ and $\epsilon_{\bar{\rm H}}$ are internal energy of Ps and $\bar{H}$ in the initial channel α_0. These cross sections are compared to each other and to other competing reactions, such as elastic scattering cross sections ($\sigma_{\rm ela}$) and Ps de-excitation cross sections ($\sigma_{\rm dex}$) for the same energy interval of the relative kinetic energy in final channel of $e^- + \bar{H}^+$. Note that the total cross sections of Ps (3s) + $\bar{H}$ (1s) are expected to be dominated by the s-wave scattering due to the small collision energy. The s-wave cross sections of Ps (1s/2s) + $\bar{H}$ (1s) are not enough to evaluate the total cross sections and we are working on inclusion of higher partial waves towards the total understanding of $\bar{H}^+$ production reactions. On the

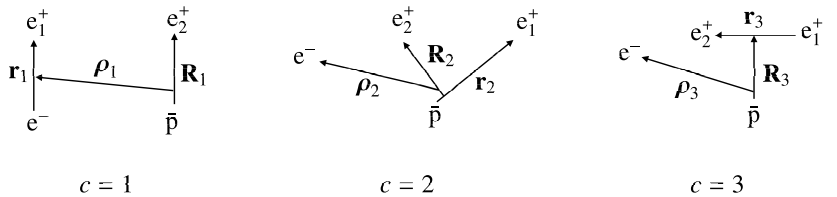

Figure 1. Three sets of Jacobian coordinate systems for intermediate states.

other hand, it is worthwhile to investigate the reaction Ps (ns) + $\bar{\mathrm{H}}$ (1s) → e^- + $\bar{\mathrm{H}}^+$ in s-wave collision for understanding the threshold behavior of the state-to-state cross sections.

Convergence of cross section against the maximum number of intermediate states is examined and we have found that cross sections almost converge with $\upsilon = 60$ ($E_{\upsilon=60} = 0.239\,68$ a.u.) from $\upsilon = 1$ (a ground state). For safety, the intermediate states are included from $\upsilon = 1$ to $\upsilon = 80$ ($E_{\upsilon=80} = 0.245\,75$ a.u.) so as to cover the collision energy sufficiently.

The $\bar{\mathrm{H}}^+$ production cross sections from Ps (1s/2s) + $\bar{\mathrm{H}}$ (1s) scattering, $\sigma_{\mathrm{ion}} = \sigma_{71}$ and σ_{72}, begin from a finite value at the threshold and show a steady value throughout the presented energy region (see figure 2 a and b). The steady behavior of the $\bar{\mathrm{H}}^+$ production cross section above the threshold in Ps (1s/2s) + $\bar{\mathrm{H}}$ (1s) (shown in figure 2 a and b) is consistent with Wigner's threshold law [50]. In the reaction Ps (1s/2s) + $\bar{\mathrm{H}}$ (1s) → e^- + $\bar{\mathrm{H}}^+$, the produced fragments attract each other through the Coulomb interaction and the speed of the relative motion is sufficiently smaller than that between the initial fragments, which results in a constant cross section above the threshold. The steady behavior of σ_{ion} is also consistent with the cross section behavior reported in a close-coupling (CC) calculation [35]. In that calculation, the $\bar{\mathrm{H}}^+$ production cross section from Ps (1s) + $\bar{\mathrm{H}}$ (1s) at the threshold was reported to show the steady behavior around 3.8 a_0^2. A similar behavior around π a_0^2 was reported in a coupled-pseudostate-approach (CPA) calculation [51,52]. For the reaction of Ps (2s) + $\bar{\mathrm{H}}$ (1s), the $\bar{\mathrm{H}}^+$ production cross section at the threshold was reported to be ∼ 60 a_0^2 in the CPA calculation [51, 52]. Note that our calculation only includes s-wave cross sections and shows smaller value than the CC and CPA calculations. This could be due to the lack of the higher partial wave contributions and the strictness of our method. A major difference in the calculation methods between this work and the CC approach is that the present one expresses the four-body correlation during the scattering by using the four-body basis functions which diagonalize the four-body Hamiltonian while the CC approach expresses the four-body correlation by linear combination of target wavefunctions. Besides, the CC calculation [35] included Ps excitation and $\bar{\mathrm{H}}^+$ formation but not $\bar{\mathrm{H}}$ virtual excitation effects.

The $\bar{\mathrm{H}}^+$ production cross section from the s-wave collision of Ps (3s) + $\bar{\mathrm{H}}$ (1s), $\sigma_{\mathrm{ion}} = \sigma_{74}$, decreases rapidly with increasing the collision energy (see figure 2 c), which is a different trend from those in Ps (1s/2s) + $\bar{\mathrm{H}}$ (1s) (see figure 2 a, b). In the reaction Ps (3s) + $\bar{\mathrm{H}}$ (1s) → e^- + $\bar{\mathrm{H}}^+$, both the initial and final fragments have similar relative speeds, which is out of the coverage of the Wigner's threshold law; therefore, the cross section $\sigma_{\mathrm{ion}} = \sigma_{74}$ does not show the steady behavior of σ_{ion}. The decrease of the cross section may be related to the fact that the inelastic cross sections are scaled by the factor of k_{i}^{-2} where k_{i} is the relative momentum in the initial.

In the low energy limit of the collision between Ps (3s) and $\bar{\mathrm{H}}$ (1s) in s-wave, the $\bar{\mathrm{H}}^+$ production cross section becomes ∼ 8.5 a_0^2. A previous calculation [23] based on a continuum distorted wave-final state (CDW-FS) theory predicted ∼ 18 a_0^2. Another previous work based on the first Born approximation [52] predicted that the $\bar{\mathrm{H}}^+$ production cross section was over 3000 a_0^2 just above the $\bar{\mathrm{H}}^+$ production threshold energy and decreased rapidly as the collision energy increased. One should note that these calculations included higher partial wave contributions. Our $\bar{\mathrm{H}}^+$ production cross section shows huge discrepancy from the first Born approximation and the behavior of the cross section against the collision energy obtained in this work is completely different from that obtained in CDW-FS. Namely, the present cross section rapidly decreases as the collision energy increases whereas the cross section in CDW-FS slowly decreases up to the collision energy ∼ 1 a.u.

The elastic scattering cross sections $\sigma_{\mathrm{ela}} = \sigma_{11}$ and σ_{22} for Ps (1s/2s) + $\bar{\mathrm{H}}$ (1s) are of the same magnitude as the $\bar{\mathrm{H}}^+$ production cross section; however, the elastic one in Ps (3s) + $\bar{\mathrm{H}}$ (1s) is around 100 times larger than the $\bar{\mathrm{H}}^+$ production cross section. Besides, the de-excitation cross section from Ps (3s) + $\bar{\mathrm{H}}$ (1s), $\sigma_{\mathrm{dex}} = \sigma_{14} + \sigma_{24} + \sigma_{34}$, is 10 times larger than the $\bar{\mathrm{H}}^+$ production cross section while the de-excitation cross section from Ps (2s) + $\bar{\mathrm{H}}$ (1s), $\sigma_{\mathrm{dex}} = \sigma_{12}$, shows smaller value than the $\bar{\mathrm{H}}^+$ production cross section.

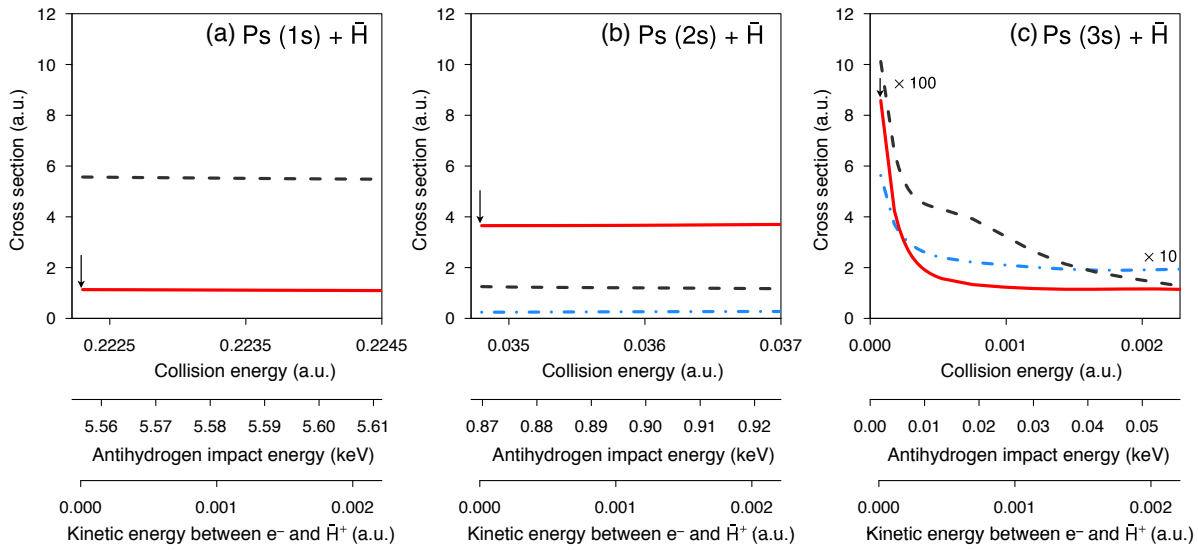

Figure 2. Cross sections of Ps (ns) + $\bar{\mathrm{H}}$ (1s) in s-wave collision are shown in (a) $n = 1$, (b) $n = 2$ and (c) $n = 3$. The arrow denotes the energy where $\mathrm{e}^- + \bar{\mathrm{H}}^+$ channel opens. Red lines are reaction cross sections $\sigma_{\mathrm{ion}} = \sigma_{7\alpha_0}$ ($\alpha_0 = 1$, 2 and 4) resulting in $\mathrm{e}^- + \bar{\mathrm{H}}^+$, black dashed lines are elastic cross sections $\sigma_{\alpha_0\alpha_0}$, and blue dotted-dashed lines are inelastic de-excitation cross sections σ_{dex} resulting in Ps ($n'l'$) + $\bar{\mathrm{H}}$ (1s) where $n' < n$. In (c) the elastic cross section should be multiplied by 100, and the inelastic de-excitation cross section by 10.

4. Summary

We have presented a four-body scattering calculation method, and applied it towards prediction of the production rate of $\bar{\mathrm{H}}^+$ in reactions between Ps (nl) and $\bar{\mathrm{H}}$ (1s). The use of intermediate states obtained by the diagonalization of the full 4-body Hamiltonian projected onto the subspace spanned by the Gaussian basis functions facilitates the description of the four-body interactions in the internal scattering region, explicitly including the rearrangement reactions. S-wave scattering cross sections between Ps (ns) and $\bar{\mathrm{H}}$ (1s) are presented. We have found that the cross section for the reaction Ps (1s) + $\bar{\mathrm{H}}$ (1s) $\rightarrow \mathrm{e}^- + \bar{\mathrm{H}}^+$ is consistent in magnitude with a previous close-coupling calculation [35]. The behavior of the cross section of the reaction Ps (2s) + $\bar{\mathrm{H}}$ (1s) $\rightarrow \mathrm{e}^- + \bar{\mathrm{H}}^+$ shows a similar trend as that of Ps (1s) + $\bar{\mathrm{H}}$ (1s) $\rightarrow \mathrm{e}^- + \bar{\mathrm{H}}^+$, both starting from a finite value and remain constant just above the threshold, which is in agreement with the Wigner's threshold law. On the other hand, the cross section of the reaction Ps (3s) + $\bar{\mathrm{H}}$ (1s) $\rightarrow \mathrm{e}^- + \bar{\mathrm{H}}^+$ shows a drastic decrease with the collision energy just above the $\mathrm{e}^- + \bar{\mathrm{H}}^+$ threshold. We have found that the threshold value of the $\bar{\mathrm{H}}^+$ production cross section from Ps (3s) + $\bar{\mathrm{H}}$ (1s) in s-wave becomes 7.8 times larger than that from Ps (1s) + $\bar{\mathrm{H}}$ (1s) and 2.3 times larger than that from Ps (2s) + $\bar{\mathrm{H}}$ (1s). It is also seen that the reaction Ps (3s) + $\bar{\mathrm{H}}$ (1s) $\rightarrow \mathrm{e}^- + \bar{\mathrm{H}}^+$ competes with predominant elastic scattering and Ps de-excitation scattering.

Acknowledgments

T.Y. would like to thank Special Postdoctoral Researcher (SPDR) program in RIKEN, Y.K. would like to thank JSPS KAKENHI Grant Number 17K05592 and 18H05461, S.J. would like to thank the Swedish Research Council (VR) for financial supports. The computation was conducted on the supercomputers ITO at Kyushu University and HOKUSAI at RIKEN.

References

[1] Amoretti M *et al.* 2002 *Nature* **419** 456
[2] Enomoto Y *et al.* 2010 *Phys. Rev. Lett.* **105** 243401
[3] The ALPHA Collaboration 2011 *Nat. Phys.* **7** 558
[4] Kuroda N *et al.* 2014 *Nat. Commun.* **5** 4089
[5] Widmann E *et al.* 2018 *Hyperfine Interact.* **240** 5
[6] Kolbinger B *et al.* 2018 *EPJ Web Conf.* **181** 01003
[7] Malbrunot C *et al.* 2018 *Philos. Trans. Roy. Soc.* A **376** 20170273
[8] Ahmadi M *et al.* 2018 *Nature* **557** 71
[9] Ahmadi M *et al.* 2017 *Nature* **548** 66
[10] Ahmadi M *et al.* 2018 *Nature* **561** 211
[11] Scherk J 1979 *Phys. Lett.* B **88** 265
[12] Cesar C L *et al.* 2005 *AIP Conf. Proc.* **770** 33
[13] The ALPHA Collaboration 2013 *Nature Commun.* **4** 1785
[14] Indelicato P *et al.* 2014 *Hyperfine Interact.* **228** 141
[15] Pérez P *et al.* 2015 *Hyperfine Interact.* **233** 21
[16] Pérez P and Sacquin Y 2012 *Classical Quant. Grav.* **29** 184008
[17] Sacquin Y 2014 *Eur. Phys. J.* D **68** 31
[18] Kellerbauer A *et al.* 2008 *Nucl. Instrum. Meth. Phys. Res.* B **266** 351
[19] Scampoli P and Storey J 2014 *Mod. Phys. Lett.* A **29** 1430017
[20] Knecht A *et al.* 2014 *Hyperfine Interact.* **228** 121
[21] Kimura M *et al.* 2015 *J. Phys.: Conf. Ser.* **631** 012047
[22] Evans C *et al.* 2018 *EPJ Web Conf.* **182** 02040
[23] Comini P and Hervieux P A 2013 *New J. Phys.* **15** 095022
[24] Comini P and Hervieux P A 2013 *J. Phys.: Conf. Ser.* **443** 012007
[25] Comini P, Hervieux P A and Biraben F 2014 *Hyperfine Interact.* **228** 159
[26] McAlinden M T, MacDonald F G R S and Walters H R J 1996 *Can. J. Phys.* **74** 434
[27] Adhikari S K 2002 *Nucl. Instrum. Methods Phys. Res.* B **192** 74
[28] Fabrikant I I and Gribakin G F 2014 *Phys. Rev.* A **90** 052717
[29] Fabrikant I I and Gribakin G F 2014 *Phys. Rev. Lett.* **112** 243201
[30] Drachman R J and Houston S K 1976 *Phys. Rev.* A **14** 894
[31] Adhikari S K and Mandal P 2000 *J. Phys.* B: *At. Mol. Opt. Phys.* **33** L761
[32] Adhikari S K 2001 *Phys. Rev.* A **63** 054502
[33] Adhikari S K and Mandal P 2001 *J. Phys.* B: *At. Mol. Opt. Phys.* **34** L187
[34] Biswas P K 2001 *J. Phys.* B: *At. Mol. Opt. Phys.* **34** 4831
[35] Blackwood J E, McAlinden M T and Walters H R J 2002 *Phys. Rev.* A **65** 030502
[36] Reeth P V and Humberston J W 2003 *J. Phys.* B: *At. Mol. Opt. Phys.* **36** 1923
[37] Zhang J Y and Mitroy J 2008 *Phys. Rev.* A **78** 012703
[38] Woods D, Ward S J and Van Reeth P 2015 *Phys. Rev.* A **92** 022713
[39] Roy S and Sinha C 2008 *Eur. Phys. J.* D **47** 327
[40] Campbell C P, McAlinden M T, MacDonald F G R S and Walters H R J 1998 *Phys. Rev. Lett.* **80** 5097
[41] Blackwood J E, McAlinden M T and Walters H R J 2002 *Phys. Rev.* A **65** 032517
[42] Froelich P, Yamashita T, Kino Y, Jonsell S, Hiyama E and Piszczatowski K 2019 *Hyperfine Interact.* **240** 46
[43] Kamimura M 1988 *Muon Catal. Fusion* **3** 335
[44] Kino Y and Kamimura M 1993 *Hyperfine Interact.* **82** 45
[45] Piszczatowski K, Voronin A and Froelich P 2014 *Phys. Rev.* A **89** 062703
[46] Zhao J and Corless R M 2006 *Appl. Math. Comp.* **177** 271
[47] Hiyama E, Kino Y and Kamimura M 2003 *Prog. Part. Nucl. Phys.* **51** 223
[48] Hiyama E 2012 *Prog. Theo. Exp. Phys.* **2012**
[49] Hiyama E and Kamimura M 2018 *Front. Phys.* **13** 132106
[50] Wigner E P 1948 *Phys. Rev.* **73** 1002
[51] McAlinden M T, Blackwood J E and Walters H R J 2002 *Phys. Rev.* A **65** 032715
[52] Swann A R, Cassidy D B, Deller A and Gribakin G F 2016 *Phys. Rev.* A **93** 052712